International Journal of Biological Macromolecules 320 (2025) 145958

Contents lists available at ScienceDirect

International Journal of Biological Macromolecules

journal homepage: www.elsevier.com/locate/ijbiomac

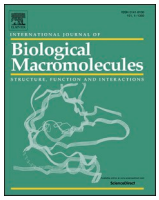

Design of fipronil and praziquantel drops using hydroxypropyl methyl cellulose E5 with superior release and penetration

Sisi Huang, Xuemei Xiao, Jing Li *

School of Pharmacy, Shenyang Medical College, Shenyang, Liaoning Province, China

ARTICLE INFO

Keywords:
Hydroxypropyl methyl cellulose E5
Cumulative drug release
Fipronil and praziquantel drops

ABSTRACT

The design of a superior release and penetration of fipronil (FPN) and praziquantel (PZQ) drops holds significant importance in the simultaneous deworming of pets both in vitro and in vivo. Herein, the application of 1,2-propanediol, azone, hydroxypropyl methyl cellulose E5 (HPMC E5) and anhydrous ethanol as osmotic promoters was investigated, with the primary objective of enhancing the drug's release and permeability. Dosages of 1,2-propanediol, azone, HPMC E5 and anhydrous ethanol were screened based on in vitro drug release and transdermal testing. The optimal prescription for the FPN and PZQ drops was obtained by using 9–11 % 1,2-propylene glycol, 69–70 % anhydrous ethanol, and 0.1–0.15 % HPMC E5. The addition of HPMC E5 can increase the in vitro cumulative release of drops and improve drug penetration into the skin. The optimal PZQ and FPN drops presented safe skin irritation, and should be stored away from strong light and high temperature.

1. Introduction

As more and more people start to keep pets, the health of pets has been widely concerned by people. Both cats and dogs are more susceptible to fleas, ticks, mites, flukes, and tapeworms. These parasites not only have an impact on the health of cats and dogs themselves, but also some of the parasites can be transmitted to humans through cats and dogs, making humans sick. For example: flea bites can cause atopic dermatitis in cats that can lead to hair loss and self-induced hair loss [1]. Fleas are the vectors of murine typhus, and humans become infected when the feces of fleas infected with Plasmodium typhus contaminate flea bites or mucous membranes. It usually presents with fever, myalgia, and headache, and in severe cases neurological symptoms may occur [2–5]. Echinococcus multilocularis causes human alveolar echinococcosis, and the adults colonize the small intestine of carnivores, mainly red foxes, cats, and dogs. Echinococcus multiloculares eggs can be excreted into the environment through the feces of the host, contaminating the environment. The larval stage is commonly found in the central nervous system of various livestock. Canine intestinal tapeworm can cause echinococcus cystosis, which is a serious zoonotic disease [6–8]. Schistosomiasis, a fluke of the genus schistosomiasis, can cause disease in humans or other mammals [9,10]. The American heterotrema can cause schistosomiasis in dogs. Clinical symptoms include diarrhea, weight loss, anorexia or anorexia, and vomiting [11]. Liver flukes can cause bile duct cancer in humans [12]. Ticks can transmit bacterial, parasitic, and viral pathogens, including anaplasmosis, babesiosis, Ehrlichiosis, borreliosis, and more [13,14]. It can infect a variety of mammals, including humans and dogs.

Parasitic infections have a significant impact on the health of pets and humans, and there are many medications available to kill fleas, ticks, mites, flukes, and tapeworms. For example, Isoxazoline is a new type of ectoparasite insecticides which consisting of four commercially available molecules: Afoxolaner, Fluralaner, Lotilaner and Sarolaner. These compounds are active on gamma-aminobutyric acid - (GABA) and glutamate-gated chloride channels. The selectivity of insect neuron receptors is better than that of mammalian receptors. This field study shows that a single topical treatment with Fluralaner can reduce clinical symptoms of atopic dermatitis in cats with flea bites [15]. Doramectin has potential antiparasitic effects on nematodes and their larvae as well as ectoparasites [16]. Pyriproxyfen has contact effect on ectoparasites [17]. This new combination of esafoxolaner, eplinomectin, and praziquantel has broad efficacy against major feline parasites, including ectoparasites and endoparasites [18].

Among them, Fipronil (FPN) is a classic drug for treating fleas and adult ticks. It belongs to benzopyrazole insecticides and is a neurotoxic insecticide that used worldwide. It interferes with the central nervous system of insects to kill pests by hindering the chloride metabolism controlled by insect y-aminobutyric acid (GABA). The main effect on

* Corresponding author.
E-mail address: dddefghijklmn@163.com (J. Li).

https://doi.org/10.1016/j.ijbiomac.2025.145958
Received 5 March 2025; Received in revised form 25 June 2025; Accepted 11 July 2025
Available online 14 July 2025

Table 1
Components of PZQ and FPN drops.

Sample	FPN (g)	PZQ (g)	Azone (g)	1,2-propanediol (g)	HPMC E5 (g)	Anhydrous ethanol (g)	Ethylparaben (g)
1	5.8	5.8	3.19	0	0	52.49	0.17
2	5.8	5.8	4.47	0	0	51.38	0.17
3	5.8	5.8	0	3.63	0	52.49	0.17
4	5.8	5.8	0	7.27	0	49.73	0.17
5	5.8	5.8	0	10.9	0	46.96	0.17
6	5.8	5.8	1.92	3.63	0	50.83	0.17
7	5.8	5.8	1.92	7.27	0	48.07	0.17
8	5.8	5.8	1.92	10.9	0	45.31	0.17
9	5.8	5.8	3.19	3.63	0	49.73	0.17
10	5.8	5.8	3.19	7.27	0	46.96	0.17
11	5.8	5.8	3.19	10.9	0	44.2	0.17
12	5.8	5.8	4.47	3.63	0	46.49	0.17
13	5.8	5.8	4.47	7.27	0	45.86	0.17
14	5.8	5.8	4.47	10.9	0	43.95	0.17
15	5.8	5.8	0	0	0	55.25	0.17
16	5.8	5.8	0	7.27	0.07	49.73	0.17
17	5.8	5.8	0	7.27	0.14	49.73	0.17
18	5.8	5.8	0	7.27	0.21	49.73	0.17
19	5.8	5.8	0	7.27	0.28	49.73	0.17
20	5.8	5.8	0	7.27	0.7	49.73	0.17
21	5.8	5.8	0	7.27	1.05	49.73	0.17
22	5.8	5.8	0	7.27	1.4	49.73	0.17

pests is stomach toxicity, with both touch and certain internal absorption [19–22]. Praziquantel (PZQ) is a deworming drug that is active against broad-spectrum flukes and tapeworms, and is mainly used to treat schistosomiasis, hepatic fluoriasis and cysticercosis. It is a heterocyclic kocinol isoquinoline derivative. PZQ had a certain effect on the activity of glutathione S-transferase (GST) in the insect, resulting in more H_2O_2 and O_2 and other reactive oxygen products gathering in the insect body. Destroy parasites by damaging the antioxidant system. Praziquantel affects the stability of Ga^{2+} in adult insects, leading to uncontrolled muscle contraction and death [24,25]. It has the advantages of high efficiency, low toxicity, easy administration and low cost [[17,23]]. If the drop contains only FPN, it can only eliminate parasites in vitro, while the only existence of PZQ can only eliminate parasites in vivo. The combination usage of FPN and PZQ in the drops can simultaneously eliminate parasites both in vitro and in vivo.

The FPN and PZQ available for purchase on the market include PZQ tablets by Sichuan Jixing Animal Pharmaceutical Co. LTD., FPN drops for external use produced by Sichuan Decheng Animal Health Co., LTD., and Boehringer Ingelheim Animal Health Co., Ltd. produces compound FPN and PZQ drops for external use at the Toulouse production plant in France under the trade name “Boraine”. However, there are no drops on the market that combine two drugs. For the first time, two separate drugs combined to produce drops, which can not only expel fleas, ear mites, ticks and other body surface pests. It also internally repels worms, such as flukes and tapeworms.

1,2-Propanediol belongs to an important multifunctional chemical enhancer in transdermal drug delivery, and its mechanism of action can be summarized by interacting with the lipids in the stratum corneum to disrupt its tightly arranged structure and improve lipid fluidity, thereby reducing skin barrier function and enhancing the permeability of active ingredients. 1,2-propanediol can also exert synergistic promotion of dissolution and moisturizing. High concentration of 1,2-propanediol can break down the stratum corneum barrier, moderate concentration enhances skin hydration and assists in ingredient diffusion, and low concentration enhances the solubility of insoluble components. As for Azone, it is a colourless liquid with a smooth feel. Azone enhances the skin transport of a wide variety of drugs including steroids, antibiotics and antiviral agents. It was reported that Azone probably exerted its penetration enhancing effects through interactions with the lipid domains of the stratum corneum [35,36]. Herein, both 1,2-propanediol and Azone were attempted to prepare FPN and PZQ drops.

Hydroxypropyl methylcellulose (HPMC), a semisynthetic cellulose derivative, was widely applied in pharmaceutical field to contribute in designing superior drug delivery systems. It has advantages in obtaining minimal susceptibility to drug interactions, consistent drug release and pH-independent behavior. The swelling and wetting of HPMC can impact both the mucoadhesive potency and the duration of interaction between the polymer and mucosal surface [37]. Among various types of HPMC, HPMC E5 has the advantages of cold water solubility, chemical inertness, stability, viscosity adjustability, metabolic inertness and safety, and it was added as matrix to regulate drug release owing to its ability to impact viscosity of system [38,39]. Most importantly, HPMC E5 with specific function to promote drug release and penetration owing to its relative lower viscosity than other HPMC was reported [37,40,41]. The main mechanism was attributed to the molecular chain of HPMC E5 attached to the methyl group of the hydrophobic part of the phospholipid bilayer and resulted in increasing membrane permeability owing to the disorder of phospholipid bilayer layer [40]. Based on these references, HPMC E5 was applied in this study by adding into the FPN and PZQ drops to increase the cumulative release of drops in vitro release experiment and improve drug penetration into the skin.

2. Materials and methods

2.1. Materials

PZQ (≥98 %) and FPN (≥97 %) were purchased from Shanghai Maclean Biotech Limited. Anhydrous ethanol (AR) were procured from Tianjin Fuyu Fine Chemica1 Co. Ltd. 1,2-propylene glycol (AR) was sourced from Tianjin Damao Chemical Reagent Factory. Factory. Peppermint oil and azone (98 %) were provided by Shandong West Asia Chemical Industry Co. Ltd. Sodium chloride (AR) was purchased from Tianjin Hengxing Chemical Reagent Manufacturing Co. Ltd. Ethyl paraben (99 %) was purchased from RON's reagent.

Instrument	Manufacturer
UV-1801 UV–Visible spectrophotometer	Beijing Beifenrayleigh Analytical Instrument (Group) Co. LTD
SYT-101 multifunctional transdermal diffuser	Yanji Aidi Zhu Technology Co. LTD.
WQF-530 Fourier transform infrared spectrometer	Beijing Beifen Rayleigh Analytical Instrument (Group) Co. LTD
BSA124S-CW One-thousandth electronic balance	Sartorius Scientific Instruments (Beijing) Co. LTD
HSC-differential Scanning calorimeter	Beijing Hengjiu Experimental Equipment Co. LTD

(*continued on next page*)

(*continued*)

Instrument	Manufacturer
W-201B digital constant temperature water bath	Changzhou Macono Instrument Co. LTD
KQ-100 V Ultrasonic cleaner	Kunshan Ultrasonic Instrument Co. LTD

2.2. Preparation of FPN and PZQ drops

The prescribed amounts of FPN and PZQ were weighed accurately, then they were added to 20 % anhydrous ethanol. Corresponding prescriptions were shown in Table 1. Afterwards, the solution was placed in the ultrasonic cleaning machine for 1 h to ensure drugs were completely dissolved. The prescribed amounts of ethyl paraben and 1.2-propylene glycol were added to the above solution. After adequate mixing, the solution was allowed to stand to facilitate the complete integration of its components. Then an appropriate volume of anhydrous ethanol was added into the above solution to reach 70 ml. Finally, 10 min ultrasonic treatment to ensure the solution's homogeneity and the solution was sealed to store. When HPMC E5 needs to be added to the solution, it would be added after adding anhydrous ethanol. Then the solution was ultrasonic treated for 0.5 h and the preparation process was complete.

2.3. In vitro drug release

All the samples were prepared according to the components in Table 1. A vertical diffusion cell apparatus featuring a partitioning artificial membrane (nylon membrane, aperture: 0.45 μm) between the supply and recipient chamber was used [33,34]. The rough side of the artificial membrane was faced to the recipient chamber and the smooth side was faced to the supply chamber to ensure an effective diffusion area of 1.54 cm^2. The medication formulations from 1 to 15 were respectively added to the supply chamber, 4 ml of a 30 % ethanol-saline solution was added into the recipient chamber and bubbles were expelled to guarantee a secure seal between the artificial membrane and the liquid interface. Afterwards, a controlled temperature and agitation rate were set, specifically maintaining a constant rate of 500 (r/min) for the recipient chamber's liquid at the temperature of 32 °C. After sample collections were conducted at predetermined intervals post-administration: 0.083, 0.167, 0.250, 0.333, 0.500, 0.667, 0.833, and 1 h, 4 ml aliquots from the recipient solution was taken out and an equivalent volume of 32 °C fresh recipient solution was supplied. Finally, the UV (UV-1801, China) absorbance of the retrieved samples was determined and the cumulative permeability Q was obtain through calculation.

2.4. Design of optimized formulation

The software used was Design-Expert 13 Version: 13.0.1.0 64-bit. The fractional factorial design was used via selection of independent and dependent variables for the preparation of formulations and evaluation of the effect of different excipients on the responses. The selected factors were concentration of 1,2-propylene glycol(A), azone(B), HPMC E5(C), absolute ethyl alcohol. The selected responses were cumulative release.

2.5. Transdermal test in rats

An appropriate amount of 20 % uratane solution was injected to healthy Wistar rat weighing 180–200 g via the abdominal cavity to induce anesthesia. After rats losing consciousness, its limbs were fastened to an anatomical board and its abdomen was facing upwards. The hair on the abdomen of the rat was first shaved with a pet shaver until the skin on the abdomen was smooth and hairless. Scissors was then used to cut the skin samples from the abdomen, to maintain skin integrity, ophthalmic scissors and fine tweezers were employed to remove mucous membranes and blood vessels. After cleaning, the skin was rinsed in the saline solution to eliminate residual material. The skin was then spread flat on a sheet of clean filter paper, and stored in the refrigerator's lower section for preservation until use. During the trial preparation phase, the skin sample was trimmed to the desired dimensions.

A vertical diffusion cell was utilized as the experimental apparatus. The treated rat skin was placed between the receiving and diffusion pools, ensuring that the epidermal layer faced the supply chamber and the dermis faced the receiving chamber. This arrangement allowed for the precise control of the effective diffusion area, which was set at 1.54 cm^2. Then, the drug solutions prepared according to formulations 3 to 5 and 14 to 18 were individually retrieved and introduced into the drug delivery reservoir. The solution was uniformly applied to the skin's surface, and 4 ml of 30 % ethanol saline was added to the receiving chamber to remove any bubbles and ensure the rats' skin was in direct contact with the liquid surface. Following continuous agitation at a temperature of 32 °C and a speed of 500 rpm, 4 ml of the receiving solution was sampled at intervals of 0.083 h, 0.167 h, 0.250 h, 0.333 h, 0.500 h, 0.667 h, 0.833 h, 1 h, 1.5 h, 2 h, 3 h, 5 h, 8 h, 12 h, 24 h, 30 h, and 48 h post-administration. An equal volume of fresh receiving solution, maintained at the same temperature, was then added, and the UV (UV-1801) absorbance was determined to calculate the cumulative permeability Q.

2.6. Infrared spectroscopic analysis

An appropriate amount of potassium bromide solid was procured and ground into powder and the powder was compressed into a tablet. A tablet was selected as a blank sample and one to two drops of the medicinal solution were dripped onto the another potassium bromide solid tablet, serving as the test sample. The blank sample was analyzed first, followed by the test sample. This procedure was repeated, sequentially assessing samples 3 to 5, and then samples14 to 18.

2.7. Differential scanning calorimetry (DSC)

A one-third portion of Poloxamer 407 was disposed within a furnace, two to three droplets of the medicinal solution were added. Then this configuration was positioned within the confines of the furnace chamber. The apparatus was configured with an initial temperature setpoint of 25 °C, culminating at 230 °C, over the duration of the analysis. The aforementioned process was reiterated, systematically testing samples 3 to 5, followed by samples 14 to 18.

2.8. Rheological experiment

The sample was tested at room temperature, shear rate from 1 to 100 s^{-1} and rotation/steady-state mode to obtain a visco-time curve. The aforementioned process was reiterated, systematically testing sample 4, followed by samples 16 to 18.

2.9. Stability study

The samples were placed under high temperature (60 °C) and strong light (4500 lx ± 500 lx) for 10 days. High humidity test was not conducted because it is exempted for liquid formulation, including drop formulation. The sample changes were observed and the absorbance of the sample was measured on day 0, day 5 and day 10.

2.10. Test for skin irritation

A 3 cm × 3 cm area of skin on the back of the rabbit was selected, and the marked skin was shaved. Three pieces were randomly selected and 0.3 ml of the prepared optimal prescription was applied to them.

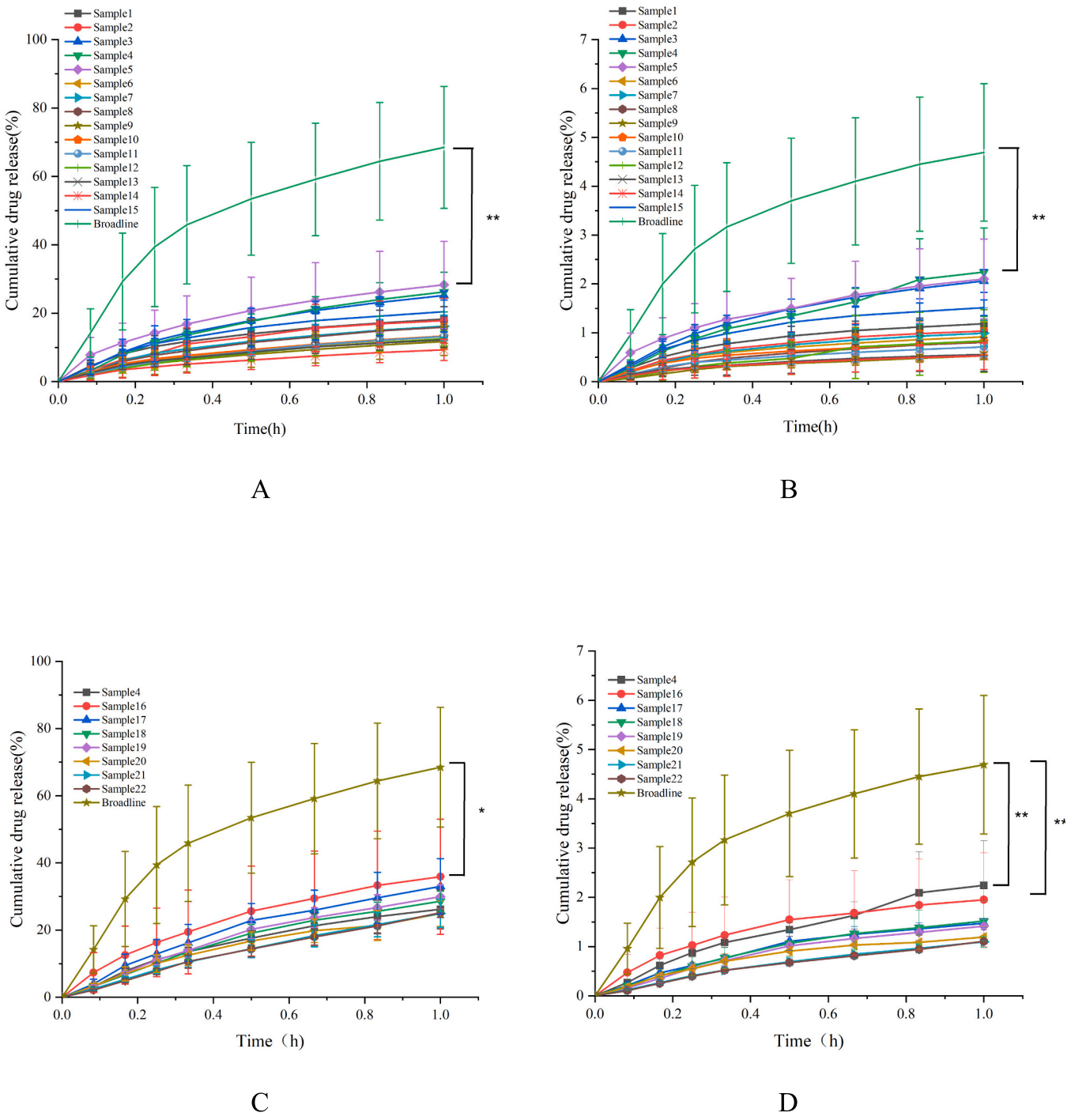

Fig. 1. A, The cumulative release of PZQ from FPN and PZQ drops with different osmotic promoters; B, The cumulative release of FPN from FPN and PZQ drops with different osmotic promoters; C, The cumulative release of PZQ from FPN and PZQ drops with different doses of HPMC E5; D, The cumulative release of FPN from FPN and PZQ drops with different doses of HPMC E5. ($n = 3$).

Another three pieces were randomly selected and the same amount of the commercially available drug Broadline was applied. Three pieces were randomly selected and 0.3 ml of the optimal prescription without the drug was applied, and the same amount of normal saline was applied to another three pieces. The skin conditions of the rabbits were observed after 1 h and 24 h.

3. Results and discussion

3.1. In vitro drug release

All the samples were prepared according to the components in Table 1. As shown in Fig. 1A, the release of sample 5 at 1 h (28.28 % ± 12.7 %) was higher than that of sample 4 (26.19 % ± 5.8 %), sample 3 (25.22 % ± 1.4 %), sample 15 (20.47 % ± 5.9 %), sample 1–2 and sample 6–14. FPN and PZQ drops with 1, 2-propanediol as osmotic

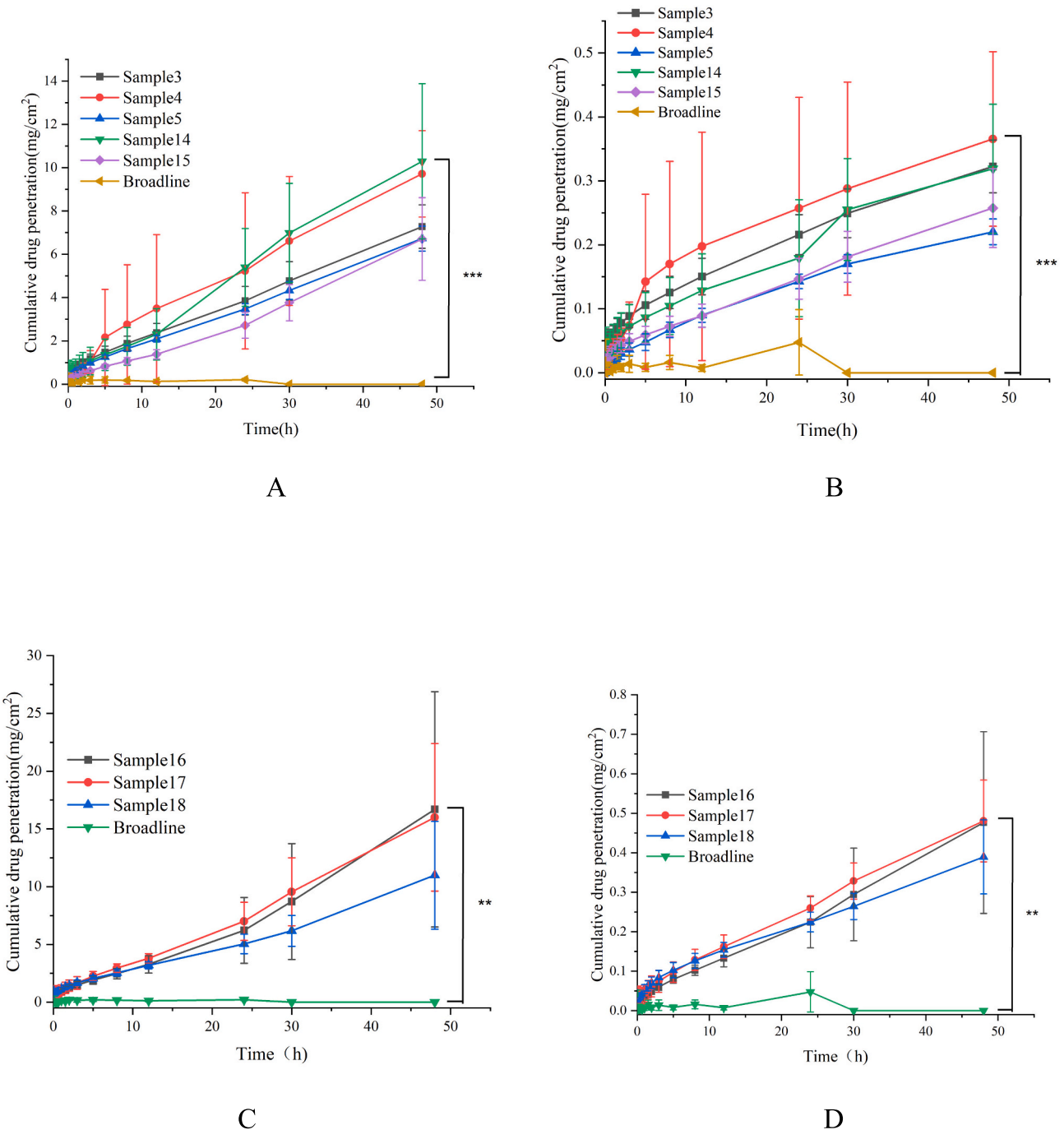

Fig. 2. A, The cumulative permeation of PZQ from PZQ and FPN drops with different osmotic promoters; B, The cumulative permeation of FPN from PZQ and FPN drops with different osmotic promoters; C The cumulative permeation of PZQ from FPN and PZQ drops with different doses of HPMC E5; D The cumulative permeation of FPN from FPN and PZQ drops with different doses of HPMC E5.(n = 3).

accelerator presented highest cumulative release of PZQ compared to the FPN and PZQ drops with azone, possibly because the effect of 1, 2-propanediol alone on PZQ was greater than that of azone alone. When combined with 1, 2-propanediol and azone, the cumulative release of 1, 2-propanediol at 7.27 g and azone at 1.92 g was higher than that of other combinations. The cumulative release of the samples without using 1, 2-propanediol and azone as osmotic accelerators was higher than that of the samples with combined use. It is possible that the interaction of the two osmotic enhancers reduced the PZQ release. In addition, the result reflected that FPN and PZQ drops with 1, 2-propanediol as osmotic accelerator presented highest cumulative release of PZQ compared to the FPN and PZQ drops with azone or the combination of 1, 2-propanediol and azone as osmotic accelerator. And the higher the content of 1,2 propylene glycol in the sample, the higher the cumulative release of PZQ.

According to Fig. 1B, the release at 1 h of sample 4 (2.24 % ± 0.9 %) was higher than the release of sample 5 (2.1 % ± 0.8 %), sample 3 (2.05 % ± 0.2 %), sample 15 (1.51 % ± 0.2 %), sample 1–2 and sample 6–14. It can be seen from the Fig. 2 that the cumulative release of F in the samples using 1, 2-propanediol alone as the osmotic accelerator was

Table 2
Design-Expert result of PZQ release and FPN release.

Source	Sequential *p*-value	Adjusted R^2	Predicted R^2
PZQ release			
Linear	< 0.0001	0.6784	0.5923
2FI	0.0105	0.7708	0.7231
FPN release			
Linear	< 0.0001	0.6835	0.5859
2FI	0.0648	0.7274	0.6346

higher than that using azone alone as the osmotic accelerator, using 1, 2-propanediol and azone in combination as the osmotic accelerator, and using neither.

According to Fig. 1C, the release at 1 h of sample 16 (35.9 % ± 17.1 %) was higher than the release of sample 17 (33.02 % ± 8.3 %), sample 19 (29.97 % ± 3.0 %), sample 18 (28.6 % ± 3.5 %), sample 4 and sample 20–22. As can be seen, the addition of HPMC E5 with a dose of 0.07 g to 0.28 g to sample 4 can promote the release of PZQ in vitro. The cumulative release of PZQ was basically unchanged when the dose of HPMC E5 in the range of 0.7 g to 0.28 g. As the dose of HPMC E5 increased, the cumulative release of drug release was inhibited, indicating that too much HPMC E5 impeded drug release due to the enhanced systemic viscosity.

As shown in Fig. 1D, The release scale of adding HPMC E5 FPN in sample 4 was small, but there was no significant difference between sample 4 and sample 16. Therefore, overall, adding a small amount of HPMC E5 can increase the release of the drug. The release at 1 h of sample 4 (2.24 % ± 0.9 %) was higher than the release of sample 16 (1.95 % ± 0.9 %), sample 17 (1.47 % ± 0.1 %), sample 18 (1.52 % ± 0.4 %), sample 19 (1.41 % ± 0.1 %) and sample 20–22. As the dose of HPMC E5 increased, the cumulative release of drug release was inhibited, indicating that too much HPMC E5 impeded drug release due to the enhanced systemic viscosity. It can be seen that the adding of HPMC E5 in the drops increased the viscosity of the drops and appropriate viscosity can increase the retention time of the drug in the skin, thereby enhancing the cumulative release of the drug and improve the insect repellent effect.

3.2. Transdermal test in rats

Initially, the result of Fig. 2A demonstrated that the addition of osmotic enhancers was crucial for achieving high PZQ permeation. Moreover, the cumulative permeability of PZQ and FPN drops with 1, 2-propanediol as osmotic promoter was higher than others before 25 h. While the cumulative permeability of PZQ and FPN drops with azone and 1, 2-propanediol as osmotic promoters was higher than that with 1, 2-propanediol alone after 25 h. These results indicated that with the increase of time, the combination of azone and 1, 2-propanediol made it easier for PZQ to penetrate into the skin possibly because the addition of azone can increase the systemic oiliness. Similarly, Fig. 2B demonstrated that the addition of osmotic enhancers was crucial for achieving high FPN permeation. Cumulative drug penetration of sample 4 (0.37 % ± 0.1 %) was higher than the cumulative drug penetration of sample 3 (0.32 % ± 0.04 %), sample 14 (0.32 % ± 0.1 %), sample 15 (0.25 % ± 0.06 %) and sample5 (0.22 % ± 0.02 %). When the dose of 1, 2-propanediol was between 3.63 g and 7.27 g, the cumulative permeability of FPN increased with the increase of the dose, which promoted the drug penetration. When 1, 2 propanediol dose between 7.27 g and 10.9 g, FPN cumulative osmotic quantity increased with the increase of the dose was reduced, inhibiting drug penetration. The cumulative permeability of the sample with 1, 2-propanediol and azone as osmotic enhancers was lower than that of the sample with 7.27 g of 1, 2-propanediol. It is possible that the interaction of the two osmotic enhancers reduced the cumulative permeability of FPN.

According to transdermal test result of Fig. 2C, cumulative drug penetration of sample 16 (16.7 % ± 10.2 %) was higher than the cumulative drug penetration of sample 17 (16.0 % ± 6.4 %), sample 18 (10.9 % ± 4.7 %) and sample 4 (10.1 % ± 1.2 %), demonstrating that the addition of low dose of HPMC E5 can increase the cumulative permeation of PZQ. The higher dose of HPMC E5 in FPN and PZQ drops impeded drug penetration through skin owing to the enhanced systemic viscosity, which was in agreement with the previous in vitro drug release result. Similarly, cumulative drug penetration of sample17 (0.48 % ± 0.1 %) was higher than the cumulative drug penetration of sample 16 (0.476 % ± 0.2 %), sample 18 (0.39 % ± 0.09 %) and sample 4 (0.37 % ± 0.1 %). The addition of HPMC E5 can increase the cumulative permeation of FPN.

It can be known from Fig. 2 that the cumulative drug penetration of samples 3–5 and 14–18 were higher than that of Broadline with significant differences. Overall, sample 16 was superior to other preparations, indicating that addition of an appropriate amount of HPMC E5 can increase the viscosity of the drops and further enhance the cumulative drug penetration of the drops and improve the insect repellent effect.

3.3. Fractional factorial design

The equation obtained according to the Central Composite Design analysis was PZQ release = 13.71 + 0.3365A-6.91B-2.49C-4.59AB-0.2916A^2+5.35B^2–1.09C^2 (A is 1,2-propylene glycol. B is azone. C is HPMC E5), and it indicated that addition of A could promote the release of PZQ, and addition of B and C could inhibit the in vitro release of PZQ. As for FPN release, the equation can be summarized as FPN release = 0.722–0.0837A-0.5785B-0.4289C-0.2394AB, and it reflected that A, B and C can not promote the release of FPN. Table 2 listed significant differences of fitted equation. Fig. 3A and B presented PZQ and FPN release effects obtained by adding A. It was clear that the maximum release amount of PZQ and FPN can be obtained when A was in the range of 6.54 g to 8.72 g, indicating that A improved drug release in this dosage range. According to Fig. 3C and D, the maximum release amount of PZQ and FPN can be achieved when B was 0 g, sufficiently demonstrated that B inhibited drug release. Fig. 3E and F reflected that in vitro drug release was gradually increased when C was in the range of 0 to 0.07 g, while decreased gradually in the range of 0.07 g to 0.21 g, remained unchanged in the range of 0.6 g to 1.4 g, demonstrating that the addition of HPMC E5 significantly impacted drug release and its dosage can not >0.6 g to obtain high drug release possibly because high dosage of HPMC E5 can enhance systemic viscosity and impeded drug release.

Fig. 4A and B showed PZQ release by adding 1,2-propylene glycol and azone. When azone was in the range of 1.788 g to 3.576 g, the release of PZQ turned out to be <15 %. The release of PZQ increased with the decrease of azone and the increase of 1,2-propylene glycol when azone was in the range of 0.15 g to 0.894 g, the release of PZQ at 15 % to 20 %. However, when azone was in the range of 0–0.15 g, the release of PZQ was >20 %. When 1,2-propanediol was in 0–4.36 g, the release of PZQ was <25 %. When 1,2-propanediol was at 4.36–10.2 g, the release of PZQ was in the range of 25–30 %. However, when 1,2-propanediol was at 10.2–10.9 g, the release of PZQ was >30 %. The maximum release of PZQ was achieved when azone was 0–0.15 g and 1,2-propanediol was 10.2–10.9 g. It is known that 1,2-propanediol can promote the release of PZQ, and azone can inhibit the release of drug.

Fig. 4C and supporting data of Fig. 4E presented PZQ release using 1,2-propylene glycol and HPMC E5. When HPMC E5 was in the 0.6–1.4 g range, the release of PZQ was <14 %. However, when HPMC E5 was in the 0–0.6 g range, the release of PZQ was greater 14 %. The release of PZQ was <16 % when 1,2-propanediol was 0–4.36 g. However, when 1,2-propanediol was at 4.36–10.9 g, the release of PZQ was >16 %. The maximum release of PZQ was achieved when HPMC E5 was 0–0.2 g and 1,2-propanediol was 4.36–10.9 g. Fig. 4D and supporting data of Fig. 4F exhibited PZQ release by adding azone and HPMC E5. When HPMC E5 was 1–1.4 g, the release of PZQ was <25 %. Then when HPMC E5 was

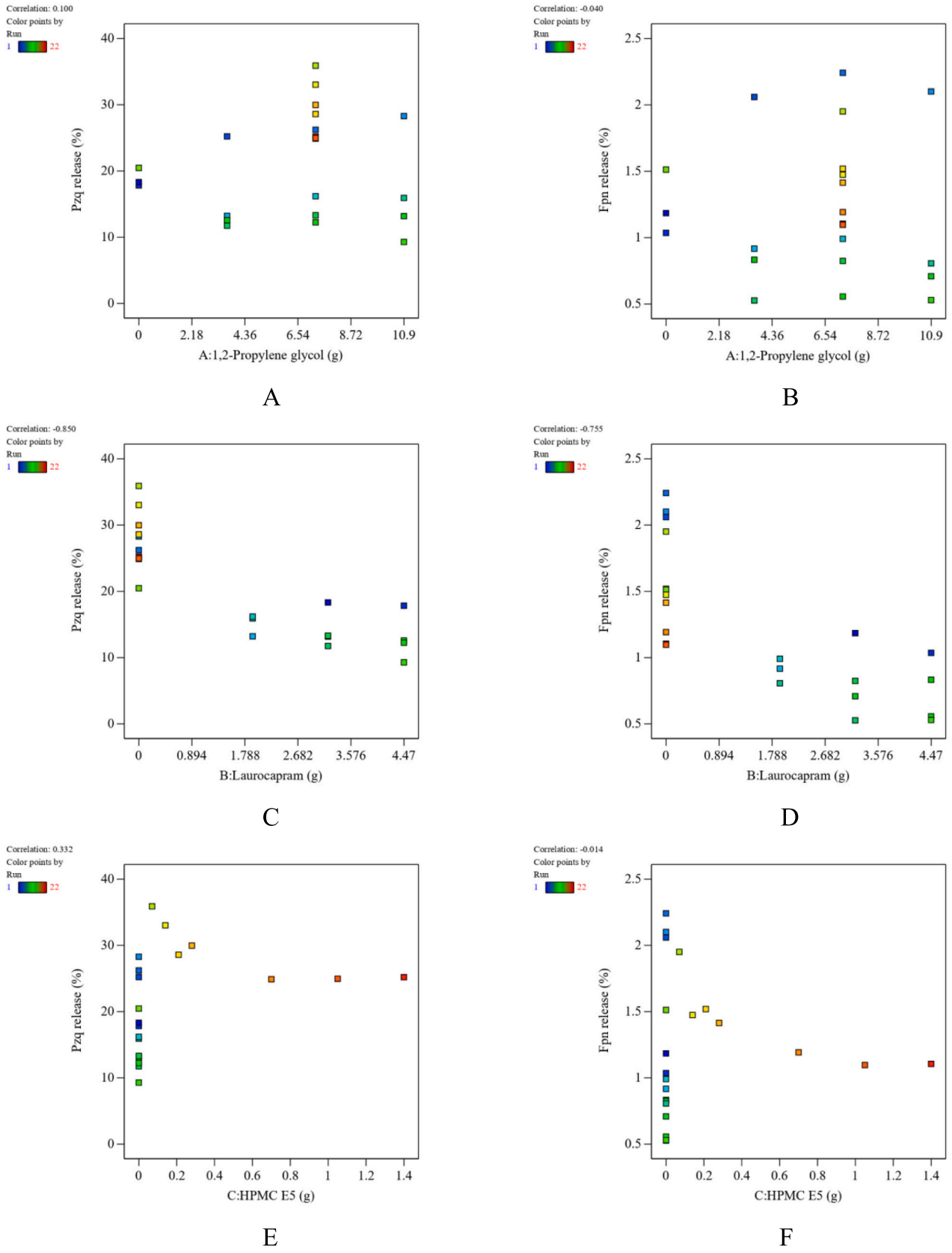

Fig. 3. Central Composite Design results of PZQ and FPN drops by analyzing each independent variable.

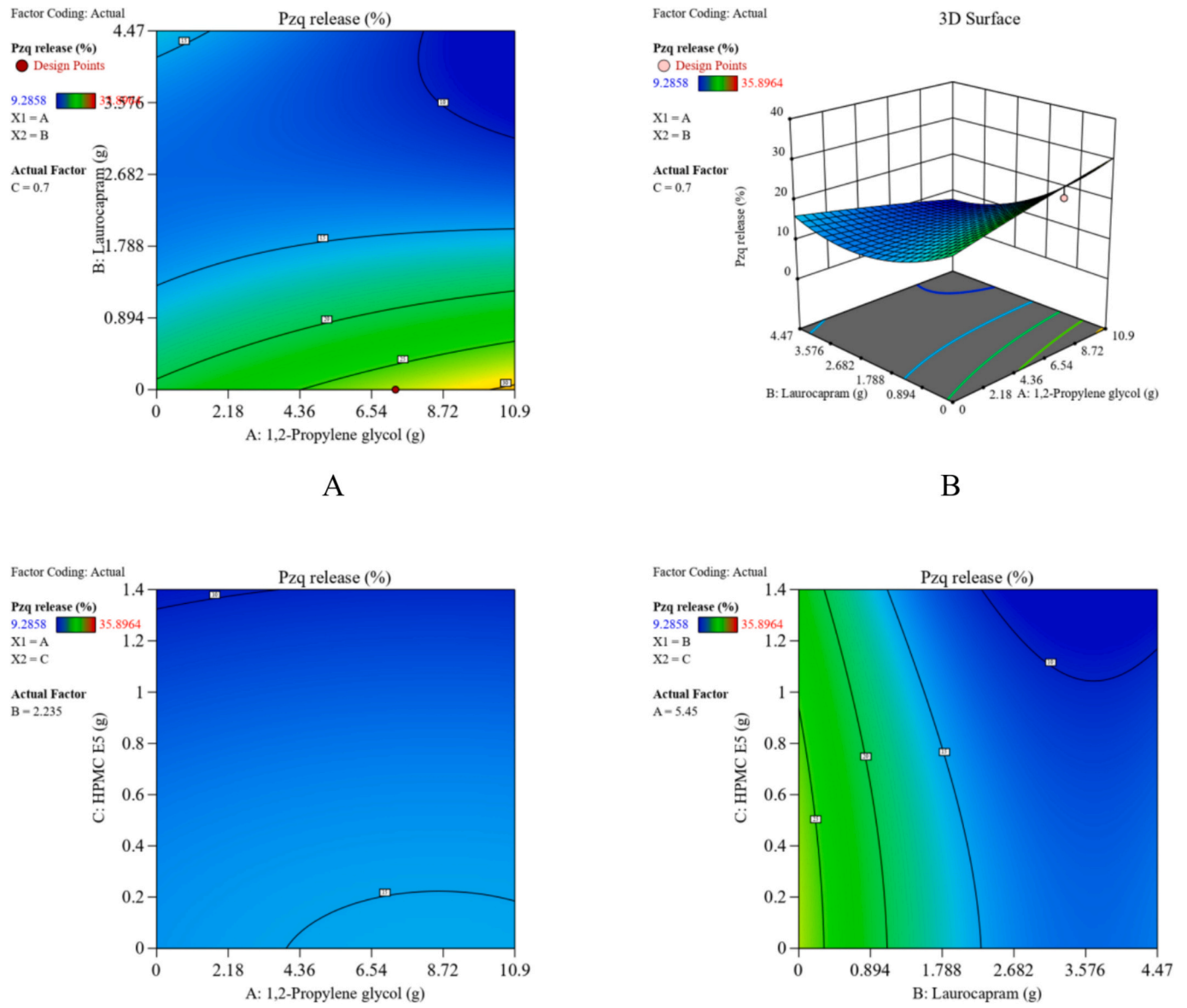

Fig. 4. Central Composite Design results of PZQ and FPN drops by presenting two-dimensional effect surface diagram and three-dimensional effect surface diagram.

0–1 g, the release of PZQ turned out to be >25 %. When azone was 0.4–4.47 g, the release of PZQ was <25 %. The release of PZQ was >25 % when azone was 0–0.4 g. The maximum release of PZQ was achieved when HPMC E5 was 0–0.8 g and azone was 0–0.4 g.

According to Fig. 5A and B, when azone was 0.894–4.47 g, the release of FPN was <1 %. The release of PZQ was >1 % when azone was 0–0.894 g. When 1,2-propanediol was 0 to 10.9 g, the release of FPN was >1 %. The maximum release was achieved when azone was 0–0.894 g and 1,2-propanediol was 0–10.9 g. Fig. 5C and supporting data of Fig. 5E showed When HPMC E5 was 0.4–1.4 g, the release of FPN was <1 %. The release was >1.2 % as HPMC E5 reached to 0–0.15 g. When 1,2-propanediol was 0–10.9 g, the release of FPN was >1 %. The release of FPN was maximal when HPMC E5 was 0–0.15 g and 1,2-propanediol was 0–2.18 g.

According to Fig. 5D and supporting data of Fig. 5F, when HPMC E5 was 0.4–1.4 g, the release of FPN was <1.5 %. The release of FPN was >1.5 % as HPMC E5 reached to 0–0.4 g. When azone was 0.894–4.47 g, the release of FPN was <1.5 %. When azone was 0–0.894 g, the release of FPN was >1.5 %. The release of FPN was maximal when HPMC E5 was 0–0.4 g and azone was 0–0.894 g. The schematic illustration of adding HPMC E5 was presented in Fig. 6.

3.4. Infrared spectroscopic analysis

Fig. 7A showed an infrared spectrogram of the PZQ and FPN drops and the PZQ raw drug. It can be seen that there was no obvious difference between the characteristic peaks of PZQ and the drop in the fourier infrared spectrogram. The results showed that PZQ had no obvious red and blue shift in the samples. The characteristic peak of PZQ at 1650 cm^{-1} indicated the stretching vibration of the C═C bond containing aromatic ring in the drug. The characteristic peak at 2855 cm^{-1} indicated a symmetric stretching vibration peak with CH_2 in the drug. The characteristic peak at 2931 cm^{-1} belonged to methylene antisymmetric stretching vibration peak.

The characteristic peak of the drug PZQ was found at 1650 cm^{-1}, and the characteristic peak of all samples was <1650 cm^{-1}, indicating that the characteristic peak was red shifted here. It may be due to the increase of conjugate effect in the sample system that the extension of intramolecular conjugate system or the increase of conjugate degree of PZQ caused red shift. It may also be due to the formation of intramolecular or intermolecular hydrogen bonds in PZQ molecules, which will increase the bond length, decrease the bond energy and reduce the vibrational frequency of the related chemical bonds, resulting in the red

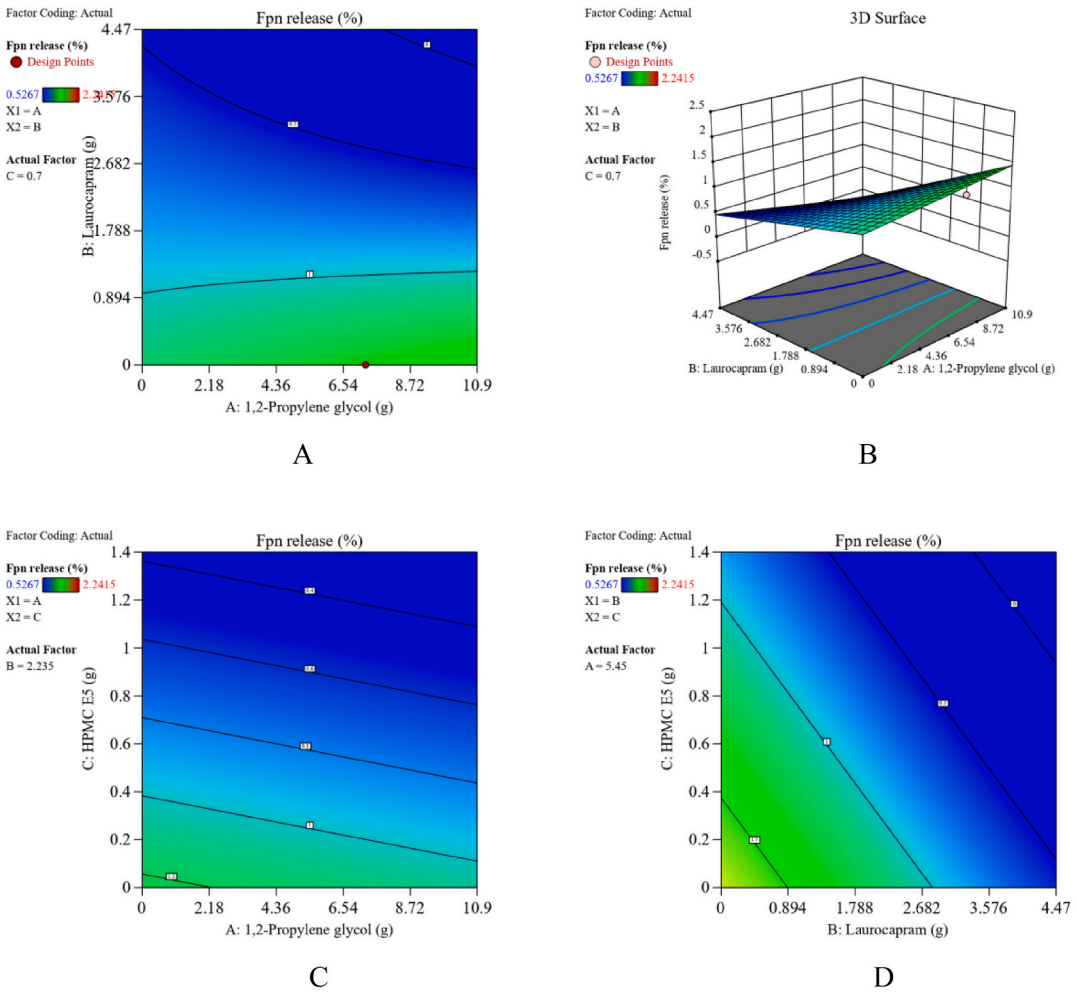

Fig. 5. Central Composite Design results of PZQ and FPN drops by presenting two-dimensional effect surface diagram and three-dimensional effect surface diagram.

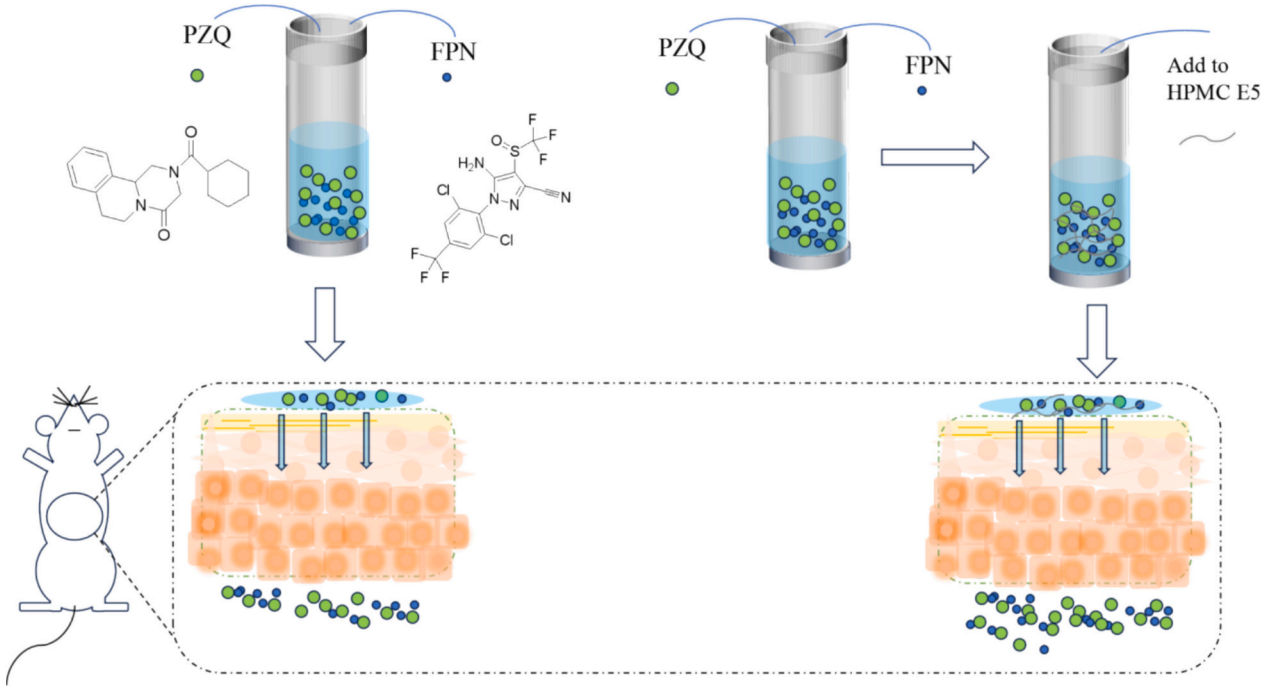

Fig. 6. Schematic illustration of HPMC E5 effect for PZQ and FPN drops.

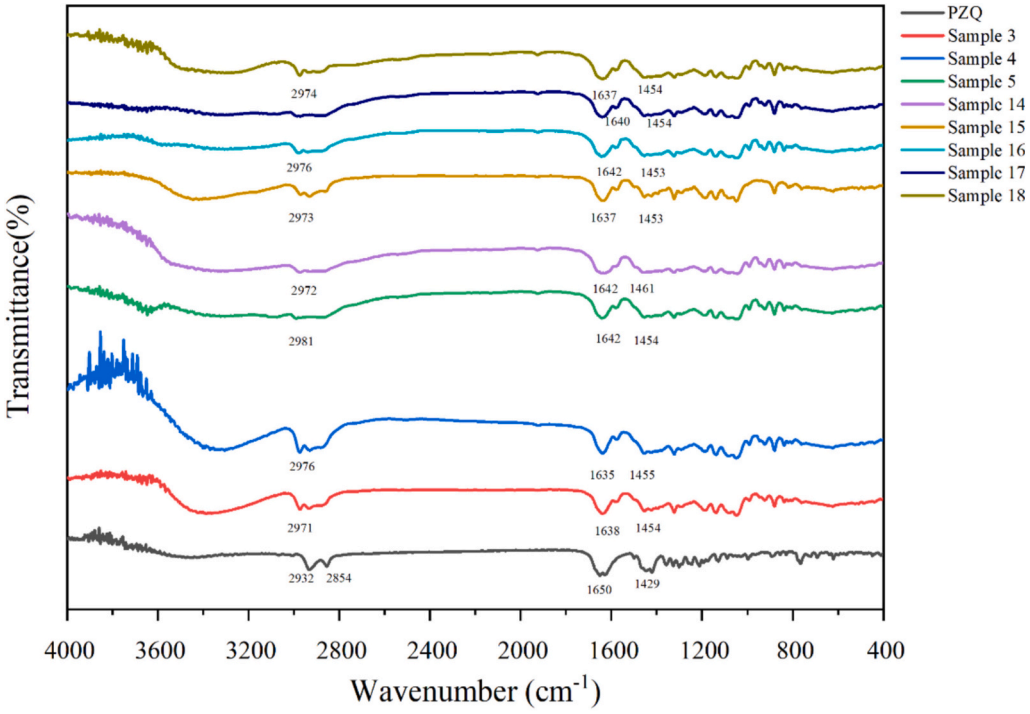

A

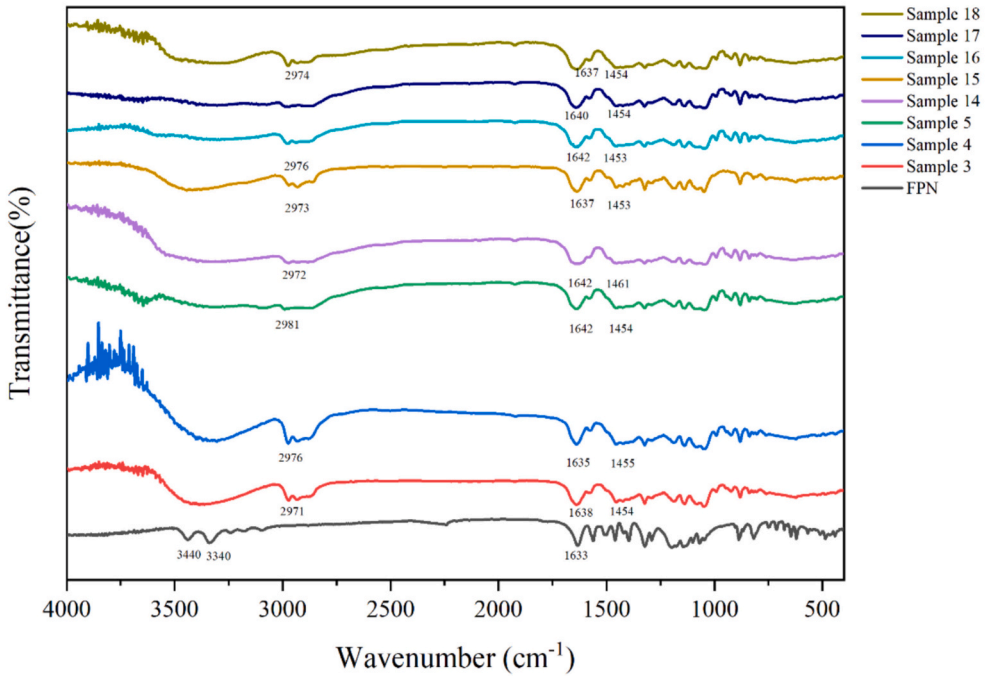

Fig. 7. IR spectra of PZQ and FPN drops, PZQ and FPN. PZQ, FPN interacted with excipients interact form hydrogen bonds.

shift of the absorption peak. The characteristic peak of the drug PZQ appeared at 1421 cm^{-1}, and the characteristic peak of all samples was larger than 1421 cm^{-1}, indicating that the characteristic peak had blue shift here. The vibrational degree of freedom of PZQ may be restricted and the vibrational frequencies of PZQ may increase. The characteristic peak of 2855 cm^{-1} was found in the drug PZQ, but not in the drops. It may be because non-pironi may have chemically reacted with PZQ or formed a compound that altered the molecular structure of PZQ, causing the functional groups or structural units that originally produced peak 2855 cm^{-1} to change, causing that peak to disappear. Or it may be that the solvent or other excipients in the drops may work together with PZQ and non-preprone to enhance the interference with peak 2855 cm^{-1} or change the presence of PZQ so that the peak can not be visible.

Fig. 7B showed an infrared spectrogram of the PZQ and FPN drops

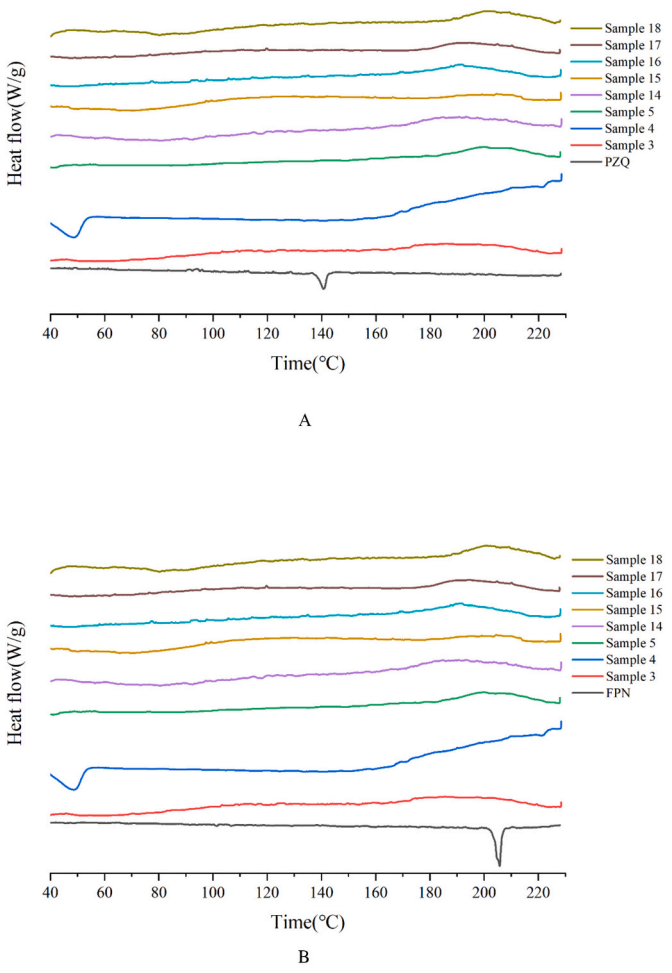

Fig. 8. DSC curves of PZQ and FPN drops, PZQ and FPN. The drug existed in the formulation with amorphous state.

and the FPN raw drug. The characteristic peak of FPN at 1633 cm^{-1} indicated that there was a stretching vibration of carbonyl group in the drug. The peak of 3340 cm^{-1} belonged to the stretching vibration peak of the drug containing the N—H bond.

The characteristic peak of drug FPN at 1633 cm^{-1} shifted blue in the sample. It is possible that because the conjugation systems of FPN molecules are destroyed or reduced, the electron separation range is reduced and the frequency of the vibration of the related chemical bonds increases, leading to absorption peak blue shifts. The characteristic peak of 3340 cm^{-1} was found in FPN, and the functional group structure of 3340 cm^{-1} peak was destroyed or changed, which resulted in the disappearance of the peak in PZQ and FPN drops. It is also possible that strong physical interactions between the two, such as hydrogen bonds, van der Waals, etc., alter the vibrational state of non-Pironi molecules, reducing the absorption strength of peak 3340 cm^{-1} to be undetectable.

3.5. DSC

As can be seen from Fig. 8A, the DSC curve presented a peak at 140.4 °C, which was the melting point of PZQ. The DSC curve of PZQ and FPN drops had no peak, which indicated that the drug existed in the preparation as a non-crystal form. As for Fig. 8B, DSC curve showed a peak at 205.4 °C that belonged to the melting point of FPN. No drug melting peak exhibited for PZQ and FPN drops, indicating that both PZQ and FPN was presented in non-crystalline form in drops [27,28].

3.6. Rheological experiment

According to Fig. 9, Sample 16 contained 0.1 % HPMC E5, Sample 17 was added 0.2 % HPMC E5 and Sample 18 consisted of 0.3 % HPMC E5. There was no obvious difference in the curve shape of the four samples. When the shear rate is between 0 and 20 s^{-1}, the viscosity increased with the increase of the shear rate, which reflected shear thickening [29–32]. When the shear rate was in the range of 20 to 120 s^{-1}, no significant change in viscosity. With the increase of shear rate, the viscosity of sample 4 minimally increased, and the viscosity of sample 17 largest increased, the difference between sample 16 and sample 18 was not obvious. It showed that when the content of HPMC E5 was 0.2 %, the viscosity turned out to be the highest. It was obvious that the addition of HPMC E5 to the PZQ and FPN drops can increase the viscosity of the system.

Fig. 9C showed the variation curves of storage modulus and loss modulus of sample 4, 16, 17 and 18 with angular frequency, where G' stands for storage modulus and G" stands for loss modulus. There was no significant difference between storage modulus and loss modulus for all samples at angular frequencies from 0 to 30 rad/s. When the angular frequency was 30–100 rad/s, the G" of sample 4 and sample17 was greater than G', indicating that the two drops remained in a liquid state. G' was greater than G" for Sample 16, indicating that the sample was in an elastic solid state. G' and G" of Sample 18 intersected at angular frequency 40 rad/s, indicating the transition of the system from an elastic liquid to an elastic solid. When the angular frequency reached 40–50 rad/s, G" was greater than G', indicating that the system was an elastic liquid. When the angular frequency was in the range of 50 to 100 rad/s, G' was greater than G", indicating that the system was an elastic solid. Adding HPMC E5 to the sample can improve the viscosity of the system.

The cumulative penetration of sample 4 was less than that of sample 18, sample 17 and sample 16. In the angular frequency range of 20 to 100 rad/s, the G' of sample 16 was always greater than G". G' was always greater than G", indicating that the system was dominated by elastic behavior. It revealed that when HPMC E5 (0.1 %) was added, a more stable elastic network structure was formed inside the drops. G' was basically unchanged, indicating that the elastic properties of the system were more stable at different angular frequencies. This reflected that the elastic network structure formed by HPMC E5 (0.1 %) had good stability and anti-interference, and the interaction between molecules was relatively solid, which will not be easily damaged by the change of external force frequency. G" decreased with increasing angular frequency, which meant that the viscosity of the system gradually decreased at high angular frequency. This change of G' and G" indicated that the drops after HPMC E5 (0.1 %) were added to form a system that was mainly stable and elastic, and the viscosity of the system was relatively weakened at high angular frequencies, and the overall elastic solid characteristics were more obvious. In the skin permeability curve, sample 16 had the highest cumulative penetration and sample 4 had the lowest cumulative permeability. This suggested that such a system facilitated drug penetration through the skin.

HPMC E5 was not added to sample 4. The G“ of sample 4 was always greater than G', indicating that the system was dominated by viscous behavior. This meant that at this time the internal structure of the system was weak, and the interaction force between the molecules was mainly expressed as the viscosity force that impeded the relative movement of the molecule. When subjected to external forces, the system dissipated energy more like a fluid through sliding between molecules, rather than storing energy like a elastomer, and overall exhibited stronger fluidity and smaller elastic recovery capacity. G" decreased with the increase of angular frequency, indicating that the viscosity of the system was more sensitive to the frequency of external force. G ‘is always smaller than G', indicating that the system's resilience was relatively weak, and the internally formed elastic network structure can not be obvious or unstable. The ability to store and retrieve energy when

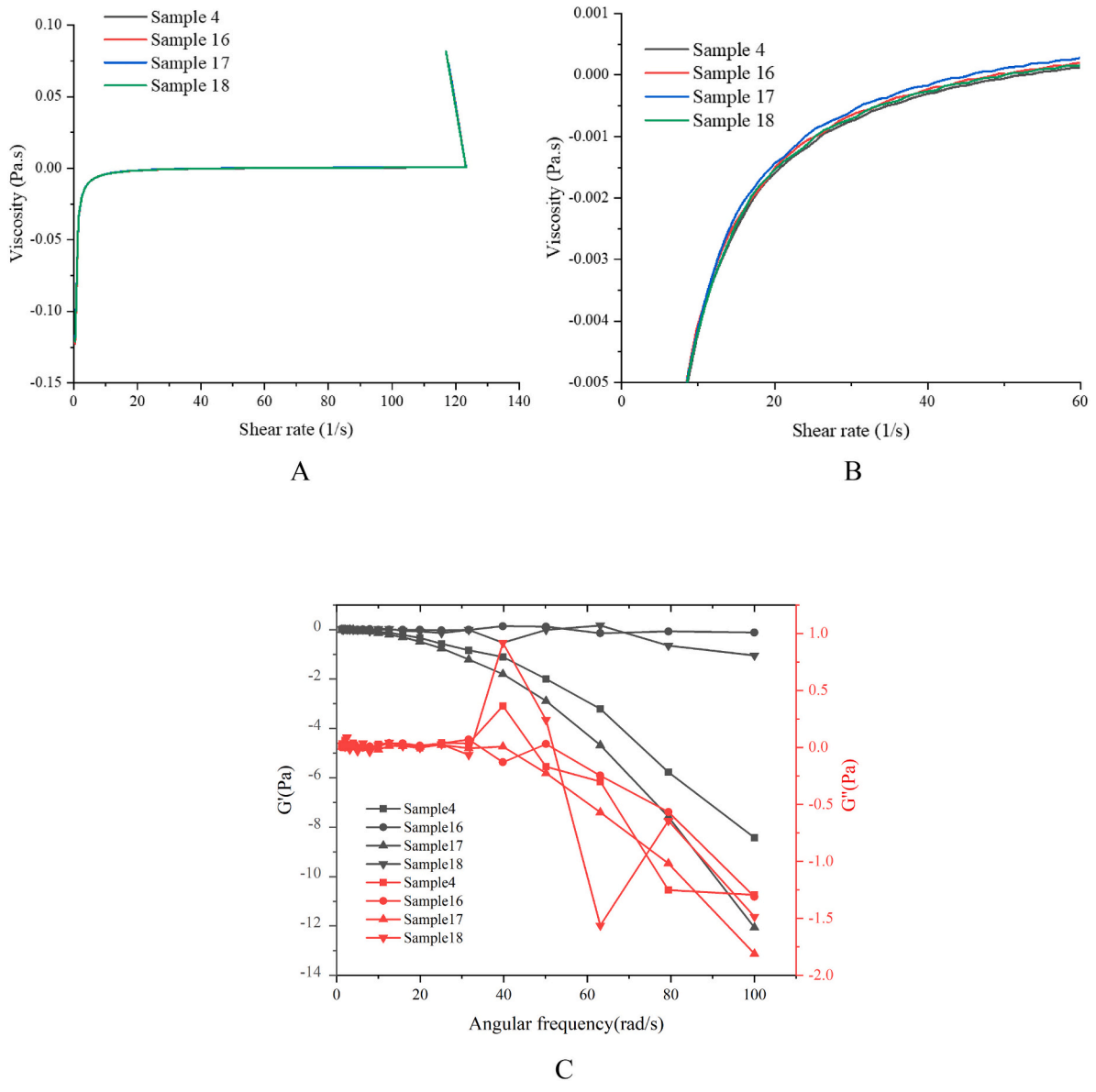

Fig. 9. A, Viscosity (Pa.s) curves of PZQ and FPN drops; B, enlarged version of viscosity in the range − 0·005 to 0.001; C, curves of storage modulus and loss modulus of sample 4, 16, 17 and 18 with angular frequency, where G' stands for storage modulus and G'' stands for loss modulus.

Table 3
The drug content of PZQ and FPN drops in the strong light experiment.

Sample	FPN content (%)			PZQ content (%)		
	0d	5d	10d	0d	5d	10d
4	98.6 ± 2.2	75.4 ± 2.1*	43.2 ± 2.3**	99.3 ± 1.1	80.2 ± 1.5*	49.2 ± 1.3**
15	99.2 ± 1.3	66.7 ± 1.6*	39.6 ± 1.9**	98.5 ± 2.0	79.1 ± 1.3*	50.3 ± 1.5**
16	98.7 ± 1.1	58.4 ± 1.7*	43.2 ± 1.5**	99.1 ± 1.3	60.6 ± 1.5*	45.6 ± 1.6**

*$P < 0.05$; **$P < 0.01$.

Table 4
The drug content of PZQ and FPN drops under high temperature conditions.

Sample	FPN content (%)			PZQ content (%)		
	0d	5d	10d	0d	5d	10d
4	99.3 ± 2.0	83.3 ± 1.1	72.2 ± 1.1*	99.4 ± 1.5	82.3 ± 1.6	77.2 ± 1.4*
15	99.0 ± 1.7	82.7 ± 1.8	71.6 ± 1.4*	99.9 ± 2.1	83.1 ± 1.5	75.3 ± 1.6*
16	99.5 ± 1.2	82.4 ± 1.3	71.2 ± 1.6*	99.0 ± 1.4	80.6 ± 1.3	76.2 ± 1.3*

*P < 0.05; **P < 0.01.

Fig. 10. A, B and C shows the skin irritation test of Broadline. A for applying the medicine; B 1 h after application; C 24 h after application. D, E, F shows the skin irritation test of sample 16. D for applying the medicine; E 1 h after application; F 24 h after application. H, I, J shows the skin irritation test of Sample16 free of drugs. H for applying the medicine; I 1 h after application; J 24 h after application. K, L, N shows the skin irritation test of normal saline. K for applying the medicine; L 1 h after application; N 24 h after application.

Table 5
Skin irritation evaluation of PZQ and FPN drops.

Conditions	Grading criteria
Skin redness	
None	0
Mild	1
Moderate	2
Severe	3
Purple-red erythema to mild eschar formation	4
Skin swelling	
None	0
Mild	1
Moderate	2
Severe(1 mm)	3
Severe(>1 mm)	4
The highest score	8

Table 6
Evaluation of skin irritation intensity.

Strength	Grading Criteria
Nonirritant	0–0.4
Mild irritation	0.5–2.9
Moderate irritation	3.0–5.9
Severe irritation	6.0–8.0

Table 7
Skin irritation score of PZQ and FPN drops.

Time	Sample16	Sample16 free of drugs	Broadline	Normal saline
1 h	0	0	0	0
24 h	0	0	0	0

exposed to external forces was limited, and it was difficult to maintain shape, and the elastic effect was not prominent. G' also decreased with the increase of angular frequency, which meant that with the increase of the external force frequency, the original weak elasticity of the system was further reduced. This may be because molecular interactions were rapidly disrupted under high-frequency external forces, making the elastic network more difficult to maintain, leading to a decrease in elasticity. Overall, the system exhibited viscosity-dominated properties without HPMC and both viscosity and elasticity decreased with angular frequency, indicating that the system lacked effective intermolecular interaction to form a stable structure and exhibited behavioral characteristics closer to those of a fluid. The minimum cumulative penetration of sample 4 indicated that the system was not conducive to drug penetration.

Sample 17 was added 0.2 % HPMC E5. The G“ of sample 17 was always greater than G', indicating that the system was still mainly viscous after adding HPMC E5 (0.2%). This may be because HPMC E5 (0.2%) had not formed a strong enough elastic network structure in the system. Or its interaction with other components in the system was weak, resulting in the adhesion force between the molecules still predominating, and when exposed to external forces, it was more likely to dissipate energy through molecular sliding, exhibiting a fluid-like behavior. G “decreased with the increase of angular frequency, indicating that the viscosity of the system was sensitive to external force frequency. G' was always less than G', indicating that the elastic properties of the system were relatively insufficient. Even when HPMC was added, problems such as the amount of addition, dissolved state or compatibility with other ingredients may make the elastic network in the system incomplete, the elastic recovery capacity was limited, and it was difficult to maintain shape when subjected to force. G' also decreased with increasing angular frequency, meaning that under high-frequency external forces, the already weak elastic structure in the system was more easily destroyed, and the elastic interaction between molecules was difficult to maintain, leading to further degradation of elasticity. The cumulative penetration of sample 17 was lower than that of sample 16, but higher than that of samples 4. The transdermal effect of this system was not as good as that of sample 16, and turned out to be better than that of the system without HPMC E5.

3.7. Stability test and skin irritation

According to the PZQ content in Table 3, it can be seen that the initial content of PZQ was >95 %, while its content on day 5 and day 10 was significantly reduced. It showed that the influence of light on PZQ was greater. The FPN content on day 5 and day 10 did not decrease significantly, indicating that light had little effect on FPN. In summary, FPN and PZQ drops should be kept away from light. Compared to the impact of strong light, high temperature showed weaker influence on the stability of PZQ and FPN drops according to Table 4. However, both PZQ and FPN contents were significantly reduced on day 10, demonstrating that PZQ and FPN drops can not be stored at high temperature conditions.

By observing the skin conditions of rabbits for 1 h and 24 h, it was found that there was no obvious edema or erythema on the skin of rabbits (see Fig. 10, Table 5, Table 6 and Table 7). The skin irritation test demonstrated PZQ and FPN drops were safe for pets to use.

4. Conclusion

FPN and PZQ drops were systemically screened, and in vitro release, transdermal penetration and viscosity of drop formulations were firstly studied. The viscosity of the droplet was characterized, and the relationship between the viscosity of the droplet and release as well as transdermal passage was deeply studied. The results indicated that the adding of HPMC E5 in the drops increased the viscosity of the drops and appropriate viscosity can increase the retention time of the drug in the skin, thereby enhancing the cumulative release and penetration of the drug and improve the insect repellent effect.

In this study, the development of FPN and PZQ drops incorporating HPMC E5 was investigated with a focus on optimizing drug release and skin penetration. The addition of HPMC E5 significantly influenced the rheological properties of the drops. When HPMC E5 was included, the relationship between the storage modulus (G') and loss modulus (G") provided valuable insights into the internal structure and viscoelastic behavior of the formulation. In cases where G' was greater than G", it indicated the formation of a relatively stable elastic-like structure, potentially beneficial for controlled drug release. Conversely, when G" was greater than G', the formulation exhibited more viscous-dominated behavior, which could also impact drug diffusion and release kinetics in different ways. Analysis of the drug release profiles demonstrated that the HPMC E5-based drops had a distinct release pattern. The presence of HPMC E5 could either retard or facilitate the release of FPN and PZQ, depending on its concentration and the resulting viscoelastic properties of the formulation. By fine-tuning the HPMC E5 concentration, we were able to achieve a more desirable release rate, ensuring a sustained and effective delivery of the drugs over time. Regarding skin penetration, the HPMC E5-containing drops showed improved performance compared to formulations without it. The optimized viscoelastic properties of the drops, influenced by HPMC E5, enhanced the ability of FPN and PZQ to penetrate the skin. This was evident from the transdermal curves, which indicated a higher cumulative amount of drugs permeating through the skin over a given period.

Overall, the use of HPMC E5 in the design of FPN and PZQ drops offers a promising approach to enhance both drug release and penetration. This research provides a solid foundation for further optimization of the formulation, taking into account factors such as the ratio of drugs, HPMC E5 concentration, and potential interactions with other excipients. Future studies could focus on in-vivo efficacy testing and exploring the long-term stability of these novel drops to translate this

research into practical applications for the treatment of relevant conditions.

CRediT authorship contribution statement

Sisi Huang: Methodology, Investigation. **Xuemei Xiao:** Methodology, Formal analysis. **Jing Li:** Writing – original draft, Project administration.

Declaration of competing interest

The authors declare that they have no known competing financial interests or personal relationships that could have appeared to influence the work reported in this paper.

Appendix A. Supplementary data

Supplementary data to this article can be found online at https://doi.org/10.1016/j.ijbiomac.2025.145958.

References

[1] M.K. Rust, The biology and ecology of cat fleas and advancements in their pest management: a review, Insects 8 (4) (2017) 118.
[2] D. Ng-Nguyen, S.F. Hii, M.T. Hoang, et al., Domestic dogs are mammalian reservoirs for the emerging zoonosis flea-borne spotted fever, caused by *rickettsia felis*, Sci. Rep. 10 (1) (2020) 4151.
[3] K.P. Legendre, K.R. Macaluso, *Rickettsia felis*: a review of transmission mechanisms of an emerging pathogen, Trop. Med. Infect. Dis. 2 (4) (2017) 64.
[4] H.H.H. Huang, R.I. Power, K.O. Mathews, et al., Cat fleas (*Ctenocephalides felis* clade 'Sydney') are dominant fleas on dogs and cats in New South Wales, Australia: presence of flea-borne *Rickettsia felis*, Bartonella spp. but absence of *Coxiella burnetii* DNA, Curr. Res. Parasitol. Vector Borne Dis. 1 (2021) 100045.
[5] L.S. Blanton, Murine typhus: a review of a reemerging flea-borne rickettsiosis with potential for neurologic manifestations and Sequalae[J], Infect Dis Rep. 15 (6) (2023) 700–716.
[6] J. Schmidberger, J. Uhlenbruck, P. Schlingeloff, et al., Dog ownership and risk for alveolar echinococcosis, Germany[J], Emerg. Infect. Dis. 28 (8) (2022) 1597–1605.
[7] P. Deplazes, R.M. Eichenberger, F. Grimm, Wildlife-transmitted Taenia and Versteria cysticercosis and coenurosis in humans and other primates[J], Int J Parasitol Parasites Wildl. 9 (2019) 342–358.
[8] A. Varcasia, C. Tamponi, F. Ahmed, et al., Taenia multiceps coenurosis: a review [J], Parasit. Vectors 15 (1) (2022) 84.
[9] H. Cridge, H. Lupiano, J.D. Nipper, et al., Efficacy of a low-dose praziquantel and fenbendazole protocol in the treatment of asymptomatic schistosomiasis in dogs [J], J. Vet. Intern. Med. 35 (3) (2021) 1368–1375.
[10] D.P. McManus, R. Bergquist, P. Cai, et al., Schistosomiasis-from immunopathology to vaccines, Semin. Immunopathol. 42 (3) (2020) 355–371.
[11] A.M. Graham, A. Davenport, V.S. Moshnikova, et al., Heterobilharzia americana infection in dogs: a retrospective study of 60 cases (2010-2019)[J], J. Vet. Intern. Med. 35 (3) (2021) 1361–1367.
[12] S.W. Kim, B.K. Jang, Toxocara canis and Fasciola hepatica co-infection leading to hepatic abscess: a case report[J], J. Korean Med. Sci. 38 (39) (2023) e323 (Published 2023 Oct 9).
[13] S. Hussain, A. Hussain, M.U. Aziz, et al., First molecular confirmation of multiple zoonotic vector-borne diseases in pet dogs and cats of Hong Kong SAR, Ticks Tick Borne Dis. 14 (4) (2023) 102191.
[14] S. Madison-Antenucci, L.D. Kramer, et al., Emerging tick-borne diseases[J], Clin. Microbiol. Rev. 33 (2) (2020) (e00083-18. Published 2020 Jan 2).
[15] A. Briand, N. Cochet-Faivre, P. Prélaud, et al., Open field study on the efficacy of fluralaner topical solution for long-term control of flea bite allergy dermatitis in client owned cats in Ile-de-France region[J], BMC Vet. Res. 15 (1) (2019) 337.
[16] E.M. Aboelela, M.A. Sobieh, E.M. Abouelhassan, et al., In-vivo and in-vitro effectiveness of three insecticides types for eradication of the tick Rhipicephalus sanguineus in dogs[J], Open Vet J. 12 (1) (2022) 44–60.
[17] M.V. Arisov, E.N. Indyuhova, G.B. Arisova, Pharmacokinetics of combination antiparasitic drug preparation for dogs and cats in the form of spot-on solution, J. Adv. Vet. Anim. Res. 6 (1) (2018) 25–32.
[18] E. Tielemans, P. Buellet, D. Young, A. Viljoen, J. Liebenberg, J. Prullage, Efficacy of a novel topical combination of esafoxolaner, eprinomectin and praziquantel against adult cat flea Ctenocephalides felis and flea egg production in cats[J], Parasite 28 (2021) 21.
[19] Z. Soualah, A. Taly, L. Crespin, et al., $GABA_A$ receptor subunit composition drives its sensitivity to the insecticide Fipronil[J], Front. Neurosci. 15 (2021) 768466.
[20] D. Poché, T. Clarke, B. Tseveenjav, Z. Torres-Poché, Evaluating the use of a low dose fipronil bait in reducing black-tailed prairie dog (Cynomys ludovicianus) fleas at reduced application rates[J], Int J Parasitol Parasites Wildl. 13 (2020) 292–298.
[21] B. Siriporn, A. Juasook, N. Neelapaijit, et al., Detection of ivermectin and fipronil resistance in Rhipicephalus sanguineus sensu lato in Maha Sarakham, Thailand[J], Vet World. 16 (8) (2023) 1661–1666.
[22] M.K. Obaid, Q. Ren, J. Luo, et al., Evaluation of fipronil efficacy and first molecular report of gamma-aminobutyric acid (GABA) gated chloride channel gene of Rhipicephalus microplus ticks in China and Pakistan[J], Vet. Parasitol. 334 (2025) 110407.
[23] Ranielly Araujo Nogueira, Maria Gabriela Sampaio Lira, Irlla Correia Lima Licá, et al., Praziquantel: an update on the mechanism of its action against schistosomiasis and new therapeutic perspectives[J], Mol. Biochem. Parasitol. 252 (2022) 0166–6851.
[24] E.G. Chulkov, E. Smith, C.M. Rohr, et al., Identification of novel modulators of a schistosome transient receptor potential channel targeted by praziquantel[J], PLoS Negl. Trop. Dis. 15 (11) (2021) e0009898.
[25] Y.H. Condeng, S. Katu, A.M. Aman, et al., Praziquantel as the preferred treatment for schistosomiasis, Int. Marit. Health 75 (1) (2024) 49–54.
[27] A. Baumgartner, O. Planinšek, Application of commercially available mesoporous silica for drug dissolution enhancement in oral drug delivery[J], Eur. J. Pharm. Sci. 167 (2021) 106015.
[28] F. Fang, M.M. Martinez, O.H. Campanella, B.R. Hamaker, Long-term low shear-induced highly viscous waxy potato starch gel formed through intermolecular double helices[J], Carbohydr. Polym. 232 (2020) 115815.
[29] M. Andersson Trojer, M. Andersson, J. Bergenholtz, P. Gatenholm, Elastic strain-hardening and shear-thickening exhibited by thermoreversible physical hydrogels based on poly(alkylene oxide)-grafted hyaluronic acid or carboxymethylcellulose [J], Phys. Chem. Chem. Phys. 22 (26) (2020) 14579–14590.
[30] M. Bolivar-Prados, Y. Hayakawa, N. Tomsen, V. Arreola, W. Nascimento, S. Riera, S. Kawakami, K. Miyaji, Y. Takeda, J. Kayashita, P. Clavé, Shear-viscosity-dependent effect of a gum-based thickening product on the safety of swallowing in older patients with severe oropharyngeal dysphagia, Nutrients 15 (14) (2023) 3279.
[31] A. Singh, K. Saitoh, Scaling relationships between viscosity and diffusivity in shear-thickening suspensions[J], Soft Matter 19 (35) (2023) 6631–6640.
[32] A.D. Crowell, T.M. FitzSimons, E.V. Anslyn, K.M. Schultz, A.M. Rosales, Shear thickening behavior in injectable tetra-PEG hydrogels cross-linked via dynamic Thia-Michael addition bonds, Macromolecules 56 (19) (2023) 7795–7807.
[33] G. Sarıbey, E. Kahraman, S. Güngör, Synthetic membrane selection for in vitro release testing (IVRT): a case study of topical mometasone furoate semi-solid dosage forms[J], Eur. J. Pharm. Sci. 203 (2024) 106934.
[34] M. Márquez Valls, A. Martínez Labrador, L. Halbaut Bellowa, D. Bravo Torres, P. C. Granda, M. Miñarro Carmona, D. Limón, A.C. Calpena Campmany, Biopharmaceutical study of triamcinolone acetonide semisolid formulations for sublingual and buccal administration, Pharmaceutics 13 (7) (2021) 1080.
[35] J. Yu, K. Wan, X. Sun, Improved transdermal delivery of morin efficiently inhibits allergic contact dermatitis, Int. J. Pharm. 530 (1–2) (2017) 145–154.
[36] A.C. Williams, B.W. Barry, Penetration enhancers, Adv. Drug Deliv. Rev. 56 (5) (2004) 603–618.
[37] O.Y. Mady, O. Dewedar, N. Abdine, H. Zaytoon, Y. Haggag, Bioadhesive behaviors of HPMC E5: comparative analysis of various techniques, histological and human radiological evidence, Sci. Rep. 14 (1) (2024) 1840.
[38] Z. Jinglin, M. Lei, M. Peihua, L. Yuan, Y. Yang, Z. QingZhu, et al., Microgel-stabilized hydroxypropyl methylcellulose and dextran water-in-water emulsion: influence of pH, ionic strength, and temperature[J], Langmuir 37 (2021).
[39] Yingyu Guo, Gege Li, Jingjing Hao, Jing Li, Design of astaxanthin cold application gel using hydroxy propyl methyl cellulose with superior release and antioxidant properties, Mater. Sci. Eng. B 299 (2024) 116982.
[40] N. Fan, Z. He, P. Ma, X. Wang, C. Li, J. Sun, Y. Sun, J. Li, Impact of HPMC on inhibiting crystallization and improving permeability of curcumin amorphous solid dispersions, Carbohydr. Polym. 181 (2018) 543–550.
[41] Z. Sun, H. Zhang, H. He, L. Sun, X. Zhang, Q. Wang, K. Li, Z. He, Cooperative effect of polyvinylpyrrolidone and HPMC E5 on dissolution and bioavailability of nimodipine solid dispersions and tablets, Asian J. Pharm. Sci. 14 (6) (2019) 668–676.